JACS
JOURNAL OF THE AMERICAN CHEMICAL SOCIETY
Article
Cite This: J. Am. Chem. Soc. 2018, 140, 5535−5543
pubs.acs.org/JACS

Tuning the Stereoselectivity and Solvation Selectivity at Interfacial and Bulk Environments by Changing Solvent Polarity: Isomerization of Glyoxal in Different Solvent Environments

Jie Zhong,[†] Marcelo A. Carignano,[‡] Sabre Kais,[§] Xiao Cheng Zeng,[†] Joseph S. Francisco,*[,†] and Ivan Gladich*[,‡]

[†]Department of Chemistry, University of Nebraska—Lincoln, Lincoln, Nebraska 68588, United States
[§]Department of Chemistry, Department of Physics and Birck Nanotechnology Center, Purdue University, West Lafayette, Indiana 47907, United States
[‡]Qatar Environment and Energy Research Institute, Hamad Bin Khalifa University, P.O. Box 31110, Doha, Qatar

Supporting Information

ABSTRACT: Conformational isomerism plays a central role in organic synthesis and biological processes; however, effective control of isomerization processes still remains challenging and elusive. Here, we propose a novel paradigm for conformational control of isomerization in the condensed phase, in which the polarity of the solvent determines the relative concentration of conformers at the interfacial and bulk regions. By the use of *state-of-the-art* molecular dynamics simulations of glyoxal in different solvents, we demonstrate that the isomerization process is dipole driven: the solvent favors conformational changes toward conformers having molecular dipoles that better match its polar character. Thus, the solvent polarity modulates the conformational change, stabilizing and selectively segregating in the bulk vs the interface one conformer with respect to the others. The findings in this paper have broader implications affecting systems involving compounds with conformers of different polarity. This work suggests novel mechanisms for tuning the catalytic activity of surfaces in conformationally controlled (photo)chemical reactions and for designing a new class of molecular switches that are active in different solvent environments.

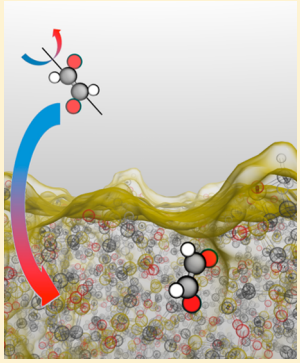

INTRODUCTION

Conformational isomerism plays a crucial role in the control of several organic synthesis and biological processes. In conformational isomerism, the structural change among isomers, also called conformers, does not involve the breaking of covalent bonds but typically a rotation around one or more single bonds.[1,2] Physicochemical processes controlled by conformational isomerism are common in nature. Diels−Alder reactions, which are often used in organic synthesis of rings, are stereospecific: the conformational structure of the reactants determines the chemical pathway and the resulting products.[3−5] Conformational changes in proteins and biomolecules are known to be associated with neurodegenerative diseases,[6,7] while in other cases they are suggested in the synthesis of novel anticancer compounds.[8] The specific conformation of reactants can lead to specific photochemical pathways[9−11] or activate hydrogen atom tunneling.[12] Conformers also serve as prochiral or chiral auxiliary molecules for the synthesis of chiral compounds.[13]

Due to the widespread occurrence of conformationally controlled processes in nature, the development of methods for the detection and separation of different conformers is highly desirable. Since conformers of the same compound can have different photochemical behavior and/or NMR response,[9,11,14,15] important advancements have been achieved in their detection. Spectroscopy combined with matrix isolation, in which gas samples are deposited on an inert matrix, has been used to investigate conformational-dependent chemistry and conformer-specific signals at low temperatures.[16−19] Conformer-specific dynamics have also been studied using vacuum UV spectroscopy.[20,21] However, the detection and isolation of a particular conformer remains nontrivial, especially in the condensed phase. Conformers are, indeed, structures lying in local minima of the free energy landscape. At ambient temperature, conformational isomers are mixed together since the rotational barrier is often comparable to the thermal energy. The ultrafast cooling that is achieved during supersonic expansion was investigated as a potential option for conformer separation in molecular beam experiments.[20−22] Cooling of macroscopic condensed phases may be an option to investigate; however, the resulting relative population of conformers upon cooling is likely to be biased by the initial population at higher temperature. These difficulties and the lack of a clear methodology to achieve conformer separation reveal a deficiency in the understanding at the molecular level of the driving mechanisms for

Received: February 13, 2018
Published: April 5, 2018

DOI: 10.1021/jacs.8b01503
J. Am. Chem. Soc. 2018, 140, 5535−5543

conformational interconversion, especially in the condensed phase.

Our capability to manipulate stereospecific processes in nature will develop to a practical level only after the formulation of a new paradigm, which calls for a deeper understanding of the fundamental mechanisms for conformer stabilization and interconversion in condensed phases and their interfaces. Recently, we observed a catalyzed *trans-to-cis* isomerization of glyoxal at the liquid water interface.[23] We pointed out an interesting and surprising property of soft interfaces in selecting specific stereo molecular structures, although this initial publication did not provide a clear molecular explanation for this phenomenon.[23] Moreover, it has been known[5] since 1962 that solvent polarity determines the chemical pathway of stereospecific reactions such as Diels–Alder reactions. The stereoselectivity of heterogeneous environments and the stereospecificity in solvents of different polarity have not been linked together so far.

Here, we provide a framework for conformer selectivity in hetero- and homogeneous solvation environments of different polarity. By using *state-of-the-art* classical and first-principles molecular dynamics, we determine the physical mechanism for the catalyzed isomerization of glyoxal at the air/liquid water interface, showing that the isomerization process is driven by the change of the molecular dipole during the conformational interconversion, matching the polar character of the solvent. By exploring different types of solvents, we observed that the relative cis/trans population at the interface and in the bulk could be tuned by properly changing the solvent polarity. In particular, a complete population inversion between the trans and cis conformers in the bulk and at the interface can be achieved by switching from an apolar to a strongly polar solvent.

The findings of this paper, even though they are based on the isomerization of glyoxal, have broader implications that are valid for a large class of compounds. Glyoxal can be considered as a prototype of any molecule having conformers of different polar character. Whenever a compound is subject to conformational isomerization with conformers of different molecular dipole, the polarity of the solvent can be used to (a) catalyze stereo structural changes and (b) stabilize and (c) selectively solvate one conformer relative to the others at the interface or in the bulk environment. Moreover, in the novel and intense research area of molecular switches,[24] glyoxal is already known to more easily convert between trans and cis conformers in the presence of a strong electrical field.[25] Here, we have shown the possibility of building a molecular switch that is sensitive to the polar characteristics of the solvent. The control of molecular motion by external stimuli is an exciting topic that gained additional attention in 2016 when the Nobel Prize in Chemistry was awarded for the design and synthesis of molecular machines.[26,27] The existence of stereoselectivity and solvation selectivity of conformers in different solvent environments presented in this work sheds further light on the catalytic activity of heterogeneous environments and opens research lines for new chemical control technologies and for the design of molecular switches in novel molecular machines.

RESULTS AND DISCUSSION

GLY Isomerization in Gas and Water. Figure 1 shows the free energy profiles for the isomerization of glyoxal (GLY) in gas, at the air/water interface, and in bulk water obtained by classical (MD) and first-principles molecular dynamics

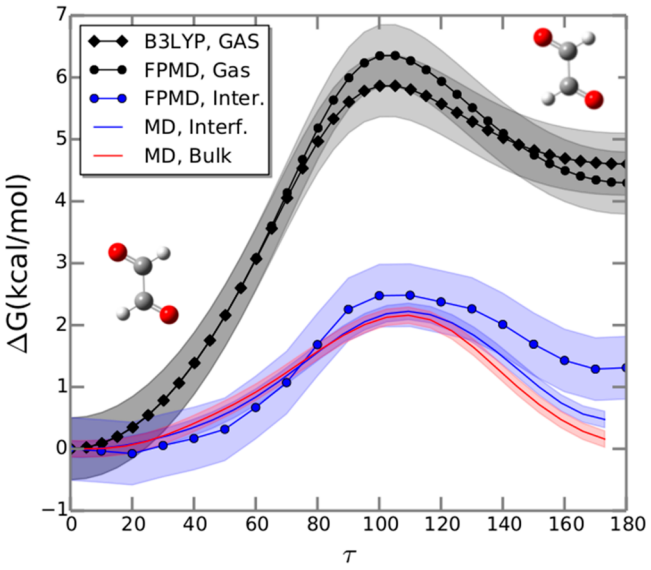

Figure 1. Isomerization profile for glyoxal in gas and liquid water. τ = 0° correspond to the trans conformer, τ = 180° to the cis one. The black lines are the gas-phase profiles, obtained at B3LYP/6-311++g(3df,3pd) electronic structure calculation (◆) and FPMD (●). The blue and red curves are the free energy profiles for GLY isomerization at the interface and in bulk water, respectively. Lines with symbols refer to results obtained from FPMD/thermodynamic integration (interface). Solid lines are those from classical MD/well-tempered metadynamics. The shaded regions represent the statistical error bar (3 standard deviation) calculated according to the reweighting method described in ref 62.

(FPMD). An isomerization transition is a rare event within the affordable time scale of MD simulations; therefore, enhanced sampling techniques were employed to bias the dynamic and extract the free energy profiles (see the Methods for more details). Similarly to what Zhu et al.[23] have reported recently, the profiles in Figure 1 show that trans (τ = 0°)-to-cis (τ = 180°) isomerization is catalyzed by the interface with respect to the gas phase. In the gas phase the barrier is about 6 kcal/mol, in agreement with previous experimental and computational works,[28−30] and this energy barrier drops to ∼2.5 kcal/mol at the surface of liquid water (Figure 1, blue lines). Our new results also show that the *trans-to-cis* barrier is further reduced to 2 kcal/mol when GLY is fully solvated in bulk water (Figure 1, red line) with an additional stabilization of the *cis* conformer. In bulk water, the barrier for the reverse transition is, indeed, 2 kcal/mol, compared to ∼1 kcal/mol in the gas phase. To summarize, while GLY is getting adsorbed at the interface and solvated in bulk water, the isomerization barrier is decreasing, and the cis isomer is stabilizing.

The isomerization profiles in Figure 1 obtained by classical MD and FPMD in Figure 1 shed some light on the physical mechanism of the catalyzed isomerization. Accurate but extremely expensive FPMD allows for more flexibility and the possibility of having electronic cloud stretching and charge transfer between atoms and molecules during the isomerization process. On the other hand, the classical force field employed here assumes fixed partial charge on each atom (Figure 2), which does not change during the simulation. Figure 2 displays the time-average Mulliken charges associated with each GLY atom in the trans, ortho, and cis configurations calculated at the FPMD level (these values are also reported in Table S1). Interestingly, the atomic charges change very little during the

DOI: 10.1021/jacs.8b01503
J. Am. Chem. Soc. 2018, 140, 5535−5543

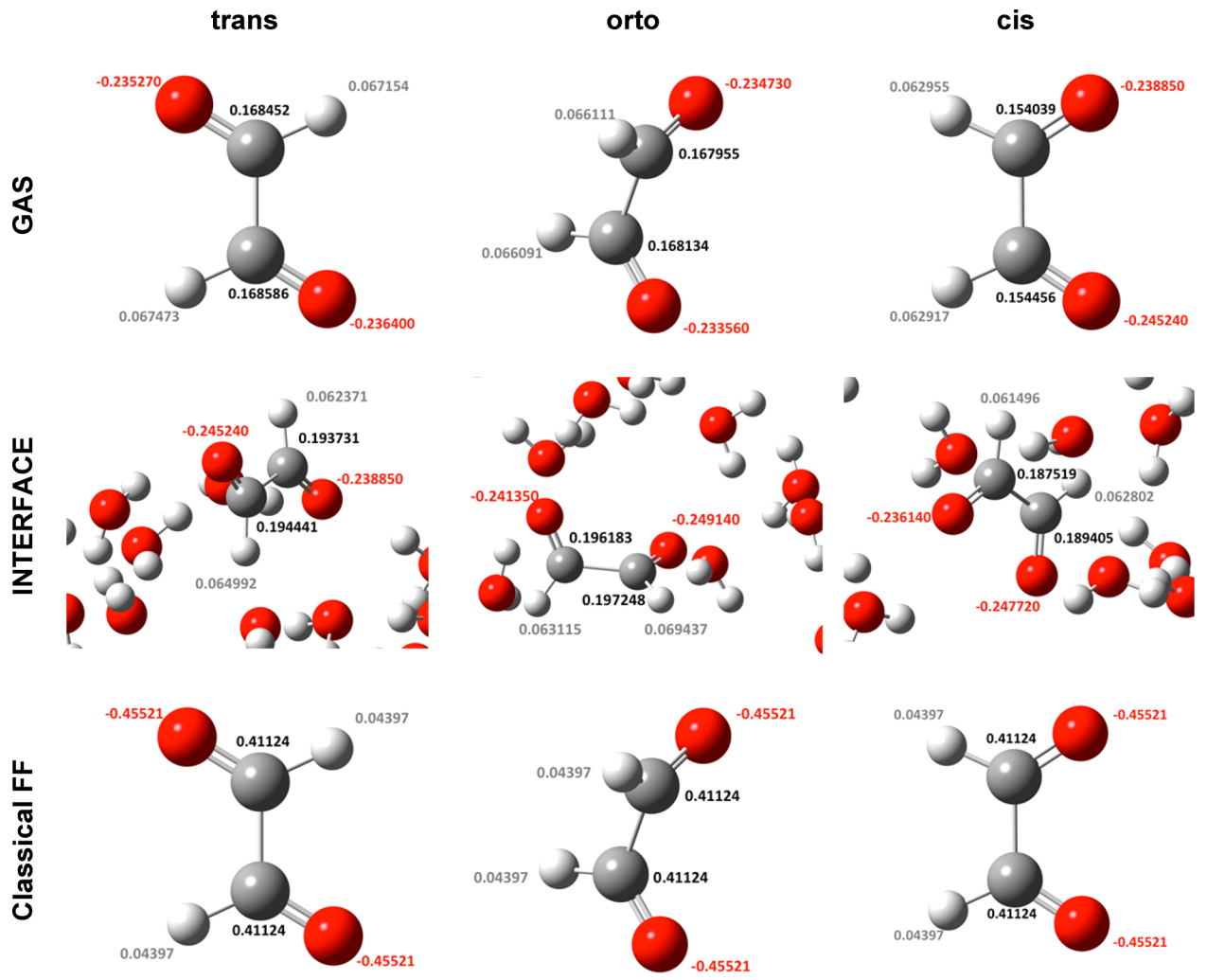

Figure 2. Partial charges of GLY at FPMD and classical MD levels, for different values of the torsion angle. Color code: red, oxygen; gray, carbon; and white, hydrogen. The top and middle rows show the time-averaged Mulliken charges at the FPMD level for GLY in the gas phase at the interface. The bottom row shows the fixed charge adopted in the classical force and obtained by RESP procedure (see Methods).

isomerization process, both in the gas and at the interface of liquid water. In the worst case, which corresponds to the carbon atoms, the relative change is smaller than 8%. Even smaller fluctuations (i.e., less than 3%) are observed for the other GLY atoms. Moreover, Figure S1 reports the HOMO orbital for GLY in the gas phase, showing that the shape of the molecular orbitals does not change during isomerization. Thus, since the electronic cloud distortion is minimal during the torsion of the molecular plane, this cannot be the physical mechanism of the catalyzed isomerization.

Figure 1 shows results from classical MD, which assumes a fixed molecular charge distribution and, thus, cannot describe the change of the induced part of the molecular dipoles at the interface.[31] This change, even if small compared to the permanent component,[31] could be relevant for the characterization of some interfacial phenomena.[32,33] Nonpolarizable force fields slightly overestimate the atomic partial charges in order to overpolarize bonds and implicitly account for average polarization effects.[34−36] However, at interfacial regions the change of the induced dipole cannot be so easily taken into account due to its change across the interfacial environment. To check the relevance of the variation of the induced dipole on the isomerization process, we also exploited classical MD using a polarizable force field. In the polarizable force field the stretching of the electronic cloud is explicitly included by allowing the atomic charges to fluctuate[37] or by using polarizable centers, such as the Drude oscillators[38,39] or point dipoles.[40,41] Polarizable force field has been shown to be able to describe the change in the induced part of the molecular dipole. Figure S2 shows the isomerization profiles when adopting a polarizable force field. The profiles are consistent with and within the statistical error bars of those obtained using a nonpolarizable fixed charge force field for both interfacial and bulk regions. This suggests that the importance of the induced component of the molecular dipole of the solvent is marginal compared to the permanent one in the conformational change process. The marginal charge redistribution within GLY during the isomerization and the minimal effect of the induced dipole on the conformational change explain why the classical force field with fixed partial charges describes comparably well the interconversion process.

Even though the charge rearrangement is minimal, there is a significant change in the molecular dipole during the isomerization process. Table 1 reports the value of the molecular dipole moment of GLY, showing a substantial change along the torsion angle. In the gas phase, trans-GLY (τ

DOI: 10.1021/jacs.8b01503
J. Am. Chem. Soc. 2018, 140, 5535−5543

Table 1. Molecular Dipole Moments during Isomerization of GLY[a]

		dipole (D)		
		trans	ortho	cis
a	GLY gas phase	0	2.18	2.74
b	GLY–liquid water interface	0.33	2.33	3.03
c	GLY, classical force field	0	3.42	4.81
	Classical Force Field Dipoles			
d	HEX	0.00 (0.00)		
e	water (TIP3P)	2.35 (2.95)[63]		
f	ACT	3.08 (2.93)[42]		
g	DMSO	4.96 (4.06)[64]		

[a]Rows a,b: Molecular dipoles for GLY in the gas phase and at the interface at the FPMD level. Row c: Dipole moment for GLY for fixed charge force field. Rows d–g: Molecular dipoles for the solvent molecules used in the classical simulation; experimental values are given in parentheses.

= 0°) has a zero dipole, which turns out to be 2.74 D in the cis form (τ = 180°). A similar trend is observed at the interface, with an even larger dipole moment (3.03 D) for cis-GLY. Table 1 reports also the GLY dipole moments in the classical force field, which are somehow a bit larger that the ones obtained by FPMD. This is not surprising since the classical force field accounts for average polarization effects by slightly over-polarizing bonds.[34−36] Nevertheless, even if small differences in the molecular dipole of GLY at classical and FPMD are present, the trend is the same: the molecular dipole increases upon conformational change from trans- to cis-GLY.

The change in the magnitude of the molecular dipole favors the interaction of GLY in water, which is a polar solvent. Figure 3 reports the radius of the solute cavity and number of hydrogen bonds (H-bonds) between GLY and water at different values of the torsion angle in bulk water. Figure 3a shows a larger solute cavity for the trans (τ = 0°) than for the cis (τ = 180°) conformers with a sharp drop at about 90–100°, which also corresponds to the transition point observed in the isomerization profile in Figure 1. The number of H-bonds between GLY oxygen and water hydrogen atoms is smaller in the trans (~1.7) than the cis (~2.1) conformers (Figure 3b), and again, a sharp variation is observed between 90 and 100°. These variations are small (about 0.03 nm for the radius and 0.4 for the H-bonds); however, the trends for both the cavity radius and the number of H-bonds are consistent. Finally, analysis of the solvation shell for GLY at the transition state (~100°) shows that the average number of H-bonds between GLY and water is 1.39 ± 0.05 at the interface and 1.94 ± 0.05 in the bulk. This suggests a lower transition-state barrier for the isomerization in bulk compared to the interface, in agreement with Figure 1.

Even though the smaller solute cavity and the larger number of H-bonds suggest a more favorable energetic environment for cis-GLY in bulk water, the intramolecular repulsions between oxygen and hydrogen atoms make the formation of the cis conformer still energetically unfavorable. In the gas phase, the trans isomer is the most common structure due to a favorable intramolecular oxygen–hydrogen (O–H) interaction that keeps the molecule planar. Because of torsion, this O–H interaction needs to be broken, resulting in the appearance of a transition point along the isomerization profile (Figure 1). However, the intramolecular O–O and H–H repulsions make the cis-GLY formed in the gas phase poorly stable, as shown by the shallow (~1 kcal/mol) *cis-to-trans* energy barrier. The presence of the solvent changes this picture dramatically. When GLY is adsorbed at the interface or, possibly, absorbed in the bulk water, the free energy penalty for the O–O and H–H repulsions is counterbalanced by the appearance of a molecular dipole. Polar solutes are more easily solvated in polar solvent due to a more favorable electrostatic interaction. Indeed, cis-GLY has a smaller solute cavity and a larger number of H-bonds with water, implying a weaker perturbation of solvent–solvent interactions and a more favorable GLY-solvent interaction, respectively. The net effect is catalysis of the isomerization process and stabilization of the cis conformer at the interface and in the bulk compared to the gas-phase case. Therefore, even if trans-GLY still remains the (free) energetically favorable isomer, formation of cis-GLY could more likely occur in liquid water.

The molecular picture that we have obtained for the isomerization of GLY in water is a dipole-driven process. The isomerization is associated with a minimal rearrangement of the electronic cloud and an important change in the molecular dipole. It is interesting to compare this with the gas-phase results of Han et al.[20] for bromocyclohexane, for which a charge delocalization was observed during the conformational change. Thus, the absence of an important distortion of the electronic cloud during the conformational change could be a peculiarity of the GLY case. Nevertheless, with or without distortion of the

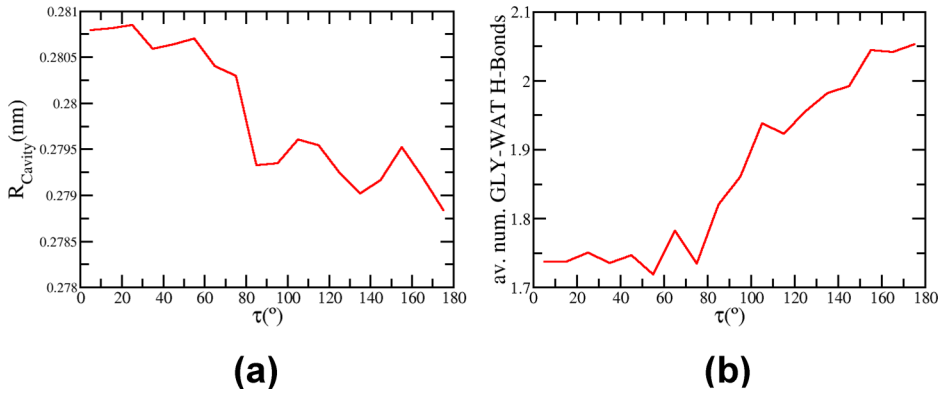

Figure 3. (a) Average cavity radius and (b) average number of H-bonds between GLY and water in bulk water radius for different values of the torsion angle. Statistics were collected over 100 ns NpT simulation with GLY fully solvated in bulk water. τ = 0° corresponds to the trans conformer, τ = 180° to the cis one.

DOI: 10.1021/jacs.8b01503
J. Am. Chem. Soc. 2018, 140, 5535–5543

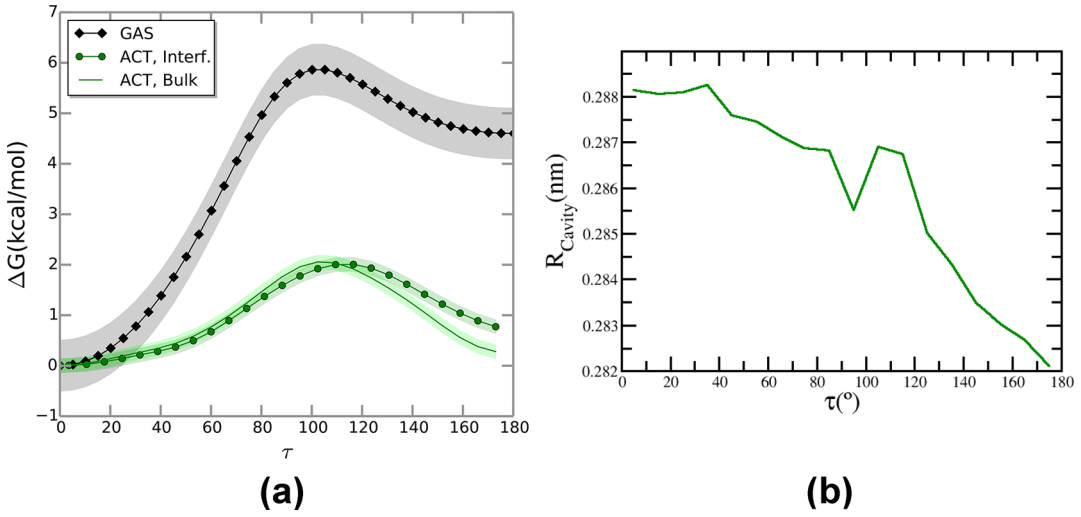

Figure 4. Isomerization profile and cavity radius for glyoxal in acetone (ACT). (a) Isomerization profile for GLY in bulk acetone (solid green line, no symbols) and at the liquid water interface (green line with ●). For reference, the isomerization profile in gas (black line with ◆) from Figure 1 is also reported. The bulk and interfacial isomerization profiles were obtained from classical NpT and NVT simulation, respectively. (b) Average cavity radius for GLY in bulk ACT as a function of the torsion angle collected over 100 ns NpT classical MD simulation. The shadow regions represent the statistical error bar (3 standard deviation) calculated according to the reweighting method described in ref 62.

electronic cloud, our results clearly link the change of the molecular dipole with the conformational transformation at the surface and in the bulk of liquid water.

GLY Isomerization in Polar, Aprotic Solvent: Acetone. To further rationalize the physics governing the conformational changes in the condensed phase, we explored the isomerization of GLY in acetone (ACT), an aprotic solvent. In ACT the hydrogen atoms are bounded to carbon and, thus, poorly polarized. As direct consequence, ACT cannot form H-bonds between its own molecules and with GLY. Nevertheless, ACT is still a polar solvent with a dipole moment in the gas phase of 2.93 D.[42]

Figure 4a shows the isomerization profiles of GLY at the interface of an ACT solvent slab and in the bulk. The isomerization behavior pretty much resembles that in water (Figure 1). Cis-GLY is stabilized in bulk and at the interface, with a *cis-to-trans* transition of ∼2 kcal/mol compared to 1 kcal/mol in the gas phase. Moreover, the isomerization is also catalyzed with a *trans-to-cis* barrier that drops to ∼2 kcal/mol. The only notable difference with the water case is that ACT is a very volatile solvent at room conditions, making its air/liquid interface very diffuse and prone to fully solvate GLY. The inspection of the trajectory shows, indeed, GLY often fully solvated in the subsurface environment (trajectory movie is available in the Supporting Information). Similar to the water case, cis-GLY has a smaller solute cavity than trans-GLY (Figure 4b). This implies a weaker perturbation of the solvent−solvent interactions, which counterbalances the free energy penalty required for intramolecular O−O and H−H repulsions. Even if ACT is a solvent incapable of making energetically favorable H-bond with the solute, the free energy penalty for having cis-GLY is partially compensated by a weaker perturbation of the solvent network around the solute, at the interface, and in the bulk.

GLY Isomerization in Polar and Apolar Solvent: Hexane and DMSO. The isomerization process was also investigated in apolar and strongly polar solvents. Figure 5 shows the free energy profiles for GLY isomerization in bulk hexane (HEX) and bulk dimethyl sulfoxide (DMSO). HEX is

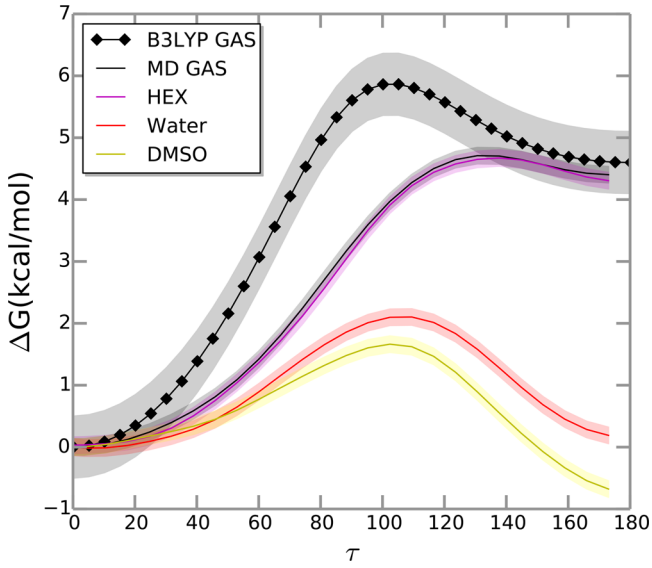

Figure 5. Isomerization profile for GLY in bulk hexane and bulk dimethyl sulfoxide, violet and yellow lines, respectively, obtained from classical MD. For reference, the figure also reports the isomerization profile in gas (black line) and bulk water (red lines) from Figure 1. The shaded regions represent the statistical error bar (3 standard deviations) calculated according to the reweighting method described in ref 62.

apolar while DMSO is a strongly polar solvent (see Table 1), and both are commonly used in laboratory practices. For the sake of comparison, Figure 5 includes the gas-phase profiles obtained at both full quantum mechanical (QM) and classical MD levels. The classical MD profile in gas shows some deviation from the one obtained at the B3LYP level because classical force fields are usually designed to work in solution and not in the gas phase. Nevertheless, the interesting point is that the isomerization profile in bulk HEX is close to the gas-phase profile obtained at the full QM level and exactly identical to the gas-phase one at the classical MD level. Figure 5 suggests

DOI: 10.1021/jacs.8b01503
J. Am. Chem. Soc. 2018, 140, 5535−5543

that the isomerization process in apolar solvent does not differ from the one in the gas phase.

The isomerization profile in DMSO displays a further catalysis of the trans-to-cis interconversion with an intriguing population inversion. Indeed, cis-GLY (τ = 180°) is now the global minimum in the free energy profile and, thus, the most stable conformer in bulk solution. The strong polarity of the solvent imposes a structural change to the conformer with higher dipole moment, fully compensating the energetic penalty for intramolecular O−O and H−H repulsions.

Figure 5 allows a comparison of the isomerization of GLY in solvents of different polarity, ranging from apolar solvent (HEX), to polar (water), and finally to strongly polar (DMSO). The molecular dipoles of these solvents are reported in Table 1. Comparing these isomerization profiles, we can extract a consistent trend between the polarity of the solvent and the catalysis of the trans-to-cis interconversion as well as the stabilization of cis-GLY: the larger is the solvent polarity, the lower is the transition barrier and stronger the cis stabilization compared to gas.

Selective Solvation. The difference in molecular dipoles among conformers naturally suggests a different surface vs bulk propensity of each isomer, depending on the polarity of the solvent. Due to the longer sampling needed to address the solvation preference, 100 ns classical MD simulations were employed, recording the value for the GLY torsion angle and trajectory in different solvent slabs. Figure 6 displays the 2D probability distribution as a function of the torsion angle τ and the Z-position of the GLY center of mass, with Z being the coordinate perpendicular to the interface. The two air/liquid interfaces of the model slab are identified with two white vertical lines. These lines are located at the positions where the solvent density drops to the 90% of its bulk value, which can be considered a reasonable marker between the bulk and the interfacial region. The solvent density profiles used to define these interfacial and bulk regions are included in Figure S3. In Figure 6 are also labeled four different regions, A, B, C, and D, which identify cis-GLY at the interface, cis-GLY in the bulk, trans-GLY at the interface, and trans-GLY in the bulk, respectively.

In the case of the HEX solvent, shown in Figure 6a, almost no cis-GLY was detected over 100 ns simulation anywhere in the slab. Table 2 reports indeed an almost zero occurrence of cis-GLY at the interface or in the bulk, regions A and B, respectively. On the other hand, Figure 6a shows a large population between τ = 0° and τ = 30°, with the trans conformer recorded for 17.92% and 52.83% of the trajectory time at the interface or in the bulk, respectively (Table 2). Thus, in apolar solvent, the conformational change from trans to cis is fully suppressed. Moreover, Figure 6a does not show any surface enhancement for GLY. Since the free energy of solvation is the logarithm of the probability distribution, this implies that once trans-GLY is adsorbed at the interface, it will be easily solvated in the bulk without crossing any energy barrier.

In water the picture becomes richer. Figure 6b and Table 2 show that the trans-GLY is still the most common conformer, both at the interface and in the bulk. This resembles the conclusions obtained from the free energy profile in Figure 1, in which the global minimum of the isomerization in water was at τ = 0° (trans-GLY) for both interfacial and bulk environments. However, in the bulk water the occurrence of cis-GLY is more than in HEX. Table 2 shows that the probability of finding cis-GLY in the bulk (region B) is larger than its corresponding value in bulk HEX, in agreement with the deeper cis-GLY minimum in the free energy profile (Figure 5). Figure 6b also shows an interesting surface enhancement for trans-GLY, identified by the red spot areas at the interfacial regions. This

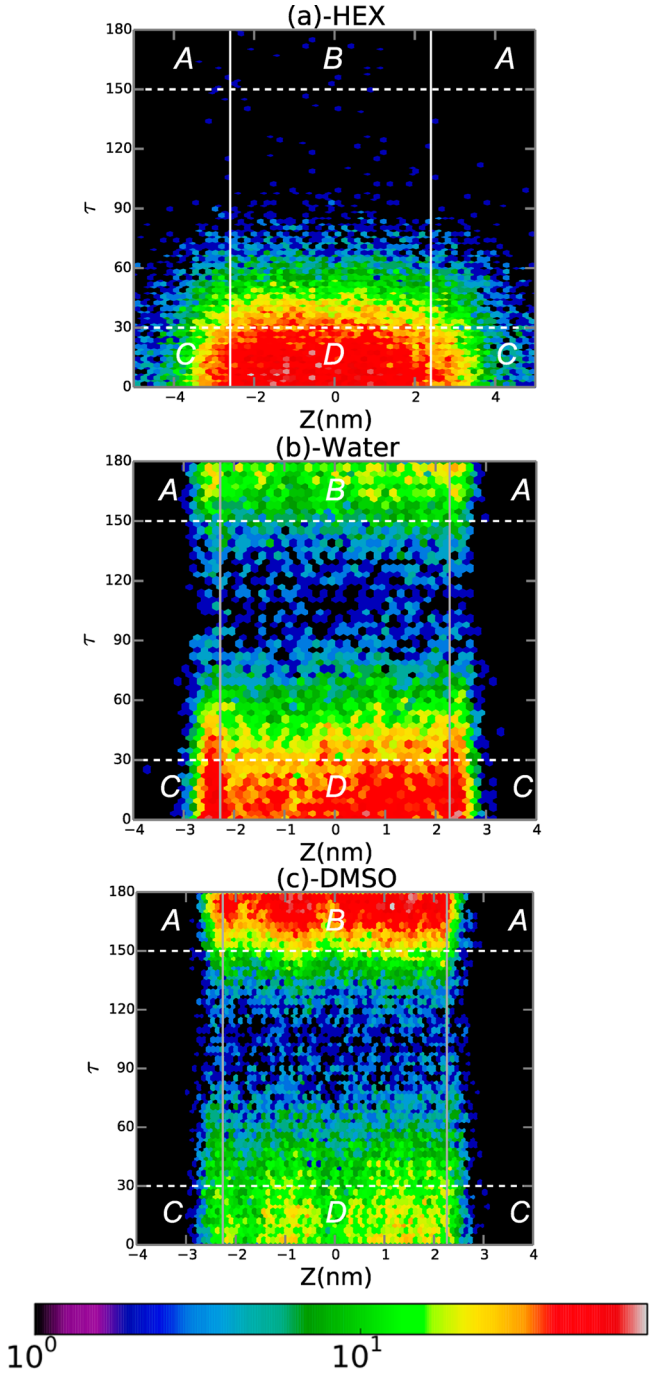

Figure 6. 2D probability distribution for the torsion angle, τ, and the center of mass position of GLY along the coordinate perpendicular to the interface, Z. Vertical gray lines are defined as 90% of the solvent density profile (see Figure S2), as marker between the bulk and interfacial region. Hotter colors imply higher population, colder colors lower. Panels (a), (b), and (c) report the distribution collecting GLY position and torsion angle over 100 ns NVT simulation in a HEX, water (nonpolarizable), water (polarizable), and DMSO slab, respectively. For visualization purposes the probability distribution was not normalized.

DOI: 10.1021/jacs.8b01503
J. Am. Chem. Soc. 2018, 140, 5535−5543

Table 2. Table of Conformer Population in Different Solvation Regions[a]

	percent population					
	A	B	C	D	cis/trans (interface) A/C	cis/trans (bulk) B/D
HEX	0.00	0.03	17.92	52.83	0.0	0.0
water	1.51	6.20	14.53	59.93	0.1	0.1
DMSO	3.79	47.58	2.34	19.81	1.62	2.4

[a]Region A: cis-GLY at the interface. Region B: cis-GLY in the bulk. Region C: trans-GLY at the interface. Region D: trans-GLY in the bulk. The last two columns report the relative concentrations cis/trans at the interface and in the bulk.

interfacial enhancement implies an energy barrier to drag trans-GLY into the bulk, which is somehow expected since trans-GLY has small (or zero) dipole, and it would prefer to stay at the interface with a polar solvent.

With a stronger polar solvent such as DMSO we obtained an opposite picture to the one obtained with water. Indeed, cis-GLY becomes the most populated structure, in the bulk and at the interface. Moreover, Figure 6c shows no surface enhancement: the strong polarity of the solvent immediately induces the conformational change and a barrierless absorption into the bulk, lowering the free energy of the system as also shown by the global minimum for cis-GLY in Figure 5.

Table 2 also displays the relative cis/trans concentration at the interface and in the bulk. In HEX, no cis-GLY is detected. In the case of water, the relative cis/trans concentration is always smaller than one, both in the bulk and at the interface. This conclusion differs from the one presented by Zhu et al.,[23] where "*cis/trans relative concentration can be enhanced in favor of the cis isomer at the interface*". This discrepancy can be rationalized by the choice of the classical force field. In this work we adopted a force field that allows isomerization of the molecule even at the classical MD level, while Zhu et al. performed classical MD constraining the torsion potential at a fixed value. This could explain the different results for water. Finally, in the case of DMSO, the relative concentration is always in favor of the cis one, especially in the bulk.

The different cis/trans relative concentrations in the bulk and at the interfacial environment of different solvents suggest a potential use of solvent polarity for controlling chemistry. An apolar or strongly polar solvent can be used to regulate the relative concentration of conformers at interfaces or in the bulk. For example, DMSO strongly suppresses trans-GLY at the interface, while cis-GLY is completely depleted on the surface of HEX. Moreover, Figures 1 and 4a suggest a selective solvation between bulk vs interfacial regions for different GLY conformers in water and ACT. Even if the relative free energy barriers for the interconversion are small (~2 kcal/mol), they are statistically relevant and sufficient to see an effect on the 2D probability distribution in Figure 6. In this work we focused on GLY as a testing prototype of conformers with different polar character: these results clearly suggest that the selective solvation can be even more marked in the case of conformers having larger differences in their molecular dipole. This stereoselectivity and solvation selectivity could be used to tune the catalytic activity of surfaces in conformationally controlled reactions.

CONCLUSIONS

Conformational isomerism is at the heart of organic synthesis and biological processes. While there have been significant advances in the detection of different conformers, especially in the gas phase, the control of isomerization processes remains highly nontrivial, especially in the condensed phase. It has been known since 1962 that the kinetics of stereoselective Diels–Alder reactions differ depending on the polarity of the solvent. Recently, a heterogeneous interfacial environment has been shown to select stereospecific molecular structures by catalyzing the isomerization process and favoring the bulk vs interfacial solvation of one conformer with respect to the other.

For the first time, in this work we link the stereoselectivity and the polarity of the heterogeneous solvent environment together, formulating a novel paradigm for conformational control in the condensed phase. Here, we determine that catalysis of the isomerization process at interfacial regions is dipole-driven: whenever the conformational change is associated with a change in the molecular dipole, the adsorbed conformer can undergo a conformational change to better match the polarity of the solvent. Depending on the solvent polarity, the isomerization process can be catalyzed while a conformer of different polarity can be selectively solvated (bulk vs interface), resulting in the segregation of the conformers. The polarity of the solvent can be chosen to regulate the relative concentration of one conformer with respect to another. As an example, we have shown that a strongly polar solvent such as DMSO suppresses trans-GLY at the interfacial environment, while an apolar solvent, such as HEX, completely depletes cis-GLY. In this study we focused on the isomerization of GLY as a testing prototype for any molecule having conformers of different polar character; therefore, the implications of these results can be appropriate for a wider class of compounds.

The stereoselectivity and solvation selectivity at heterogeneous environments of different polarity could eventually lead to the identification of new mechanisms for tuning the catalytic activity of surfaces in conformationally controlled (photo)-chemical reactions. Moreover, the possibility of controlling the conformational change opens interesting possibilities for using conformers as molecular switches,[24] in which the switch is triggered by environmental stimuli (e.g., changes in temperature, light, electric current, pH, presence of a ligand, etc.). Here we have shown the possibility of building a molecular switch which can be activated in response to a change in the solvent environment. The control of molecular motion by external stimuli is a hot research area, which gained additional attention by the 2016 Nobel Prize in Chemistry awarded for the design and synthesis of molecular machines.[26,27] Our results should encouraging future work to further explore the effects of other environmental stimuli affecting the conformer selectivity on condensed substrates of different polarity.

METHODS

First-principles and classical molecular dynamics simulations were performed to determine the isomerization profiles and to investigate the solvation environment of GLY at the interface and bulk of different solvents.

In FPMD the dynamics of the system is driven by forces calculated *on-the-fly* using density functional theory, which makes this type of calculations very accurate (but also extremely expensive). We employed FPMD simulations using the C2PK MD package.[43] Classical MDs based on predefined interaction potentials, i.e., force field, are

DOI: 10.1021/jacs.8b01503
J. Am. Chem. Soc. 2018, 140, 5535–5543

computationally cheaper, allowing longer sampling times compared to the ones needed for the investigation of solvation propensity and environment. Here, the GAFF[44,45] force field was adopted to model the solvent−solvent and solute−solvent interactions in our system and the torsion of the molecular plane of GLY. This force field has been already used to study the adsorption of different surfactants on different liquid solvents.[34,46,47] According to GAFF practice, we employed the TIP3P model[48] to describe the water phase. ACT, HEX, and DMSO were also described using GAFF nonbonding parameters and RESP[49] charges. We also exploited polarizable simulation using the SWM4-NDP water model.[39,50,51] Classical MD simulations were performed using the GROMACS 2016.3 MD package.[52]

For computing the isomerization profile, GLY was initially placed on the top of a previously equilibrated slab of water, ACT, HEX, and DMSO. GLY was kept at the interface by applying a wall potential, acting only when the molecule tried to escape the interfacial region. In this way, GLY was kept at the interface without affecting its solvation environment. For the isomerization in bulk solvent, a full periodic boundary condition (PBC) in a constant pressure (NpT) ensemble was employed.

Thermodynamic integration[53] and (well-tempered) metadynamics[54−57] as implemented in PLUMED 2.3[58] were used to bias the torsion angle, τ, of the GLY molecular plane during the FPMD and classical MD, respectively, and, afterward, to reconstruct the isomerization free energy profile. The convergence of the free energy profiles was verified by observing the diffusivity of the collective variable and comparing well-tempered with standard metadynamics results. Electronic structure calculations were employed using Gaussian09[59] at the B3LYP/6-311++g(3df,3pd) level.[60,61] The cavity radius was calculated by spanning a switching delta-like function over different values of the cutoff distance starting from the center of mass of GLY, using the coordination collective variable implemented in PLUMED 2.3.

Full details about the analysis and computational setup of the classical and FPMD simulations are reported in the Supporting Information.

■ ASSOCIATED CONTENT

Supporting Information

The Supporting Information is available free of charge on the ACS Publications website at DOI: 10.1021/jacs.8b01503.

Molecular dynamics setup and benchmark, including Figures S1−S3 and Tables S1 and S2 (PDF)

GLY-ACT trajectory movie (AVI)

■ AUTHOR INFORMATION

Corresponding Authors

*jfrancisco3@unl.edu

*igladich@hbku.edu.qa

ORCID

Marcelo A. Carignano: 0000-0001-8345-7724

Sabre Kais: 0000-0003-0574-5346

Xiao Cheng Zeng: 0000-0003-4672-8585

Joseph S. Francisco: 0000-0002-5461-1486

Ivan Gladich: 0000-0003-0929-3439

Notes

The authors declare no competing financial interest.

The data that support the findings of this study are available from the corresponding author upon reasonable request.

■ ACKNOWLEDGMENTS

For HPC resources and services we acknowledge the Research Computing group in Texas A&M University at Qatar, founded by the Qatar Foundation for Education, Science and Community Development and the Holland Computing Center at University Nebraska-Lincoln. I.G. thanks Prof. A. Laio, Prof. F. Pietrucci, and Dr. Ross D. Hoehn for their thoughtful reading and discussion, which greatly improved this manuscript.

■ REFERENCES

(1) Chhabra, N.; Aseri, M. L.; Padmanabhan, D. *Int. J. Appl. Basic Med. Res.* **2013**, *3*, 16.

(2) IUPAC. *Compendium of Chemical Terminology*; International Union of Pure and Applied Chemistry, 2006.

(3) Beniwal, V.; Kumar, A. *Phys. Chem. Chem. Phys.* **2017**, *19*, 4297.

(4) Kobuke, Y.; Sugimoto, T.; Furukawa, J.; Fueno, T. *J. Am. Chem. Soc.* **1972**, *94*, 3633.

(5) Berson, J. A.; Hamlet, Z.; Mueller, W. A. *J. Am. Chem. Soc.* **1962**, *84*, 297.

(6) Gerben, S. R.; Lemkul, J. A.; Brown, A. M.; Bevan, D. R. *J. Biomol. Struct. Dyn.* **2014**, *32*, 1817.

(7) Chiti, F.; Dobson, C. M. *Annu. Rev. Biochem.* **2006**, *75*, 333.

(8) Murray, B. S.; Menin, L.; Scopelliti, R.; Dyson, P. J. *Chem. Sci.* **2014**, *5*, 2536.

(9) Kim, M. H.; Shen, L.; Tao, H.; Martinez, T. J.; Suits, A. G. *Science* **2007**, *315*, 1561.

(10) Park, S. T.; Kim, S. K.; Kim, M. S. *Nature* **2002**, *415*, 306.

(11) Bartocci, G.; Spalletti, A. *J. Phys. Chem. A* **2002**, *106*, 7068.

(12) Mardyukov, A.; Quanz, H.; Schreiner, P. R. *Nat. Chem.* **2017**, *9*, 71.

(13) Stetsovych, O.; Švec, M.; Vacek, J.; Chocholoušová, J. V.; Jančařík, A.; Rybáček, J.; Kosmider, K.; Stará, I. G.; Jelínek, P.; Starý, I. *Nat. Chem.* **2017**, *9*, 213.

(14) Wu, J.; Lorenzo, P.; Zhong, S.; Ali, M.; Butts, C. P.; Myers, E. L.; Aggarwal, V. K. *Nature* **2017**, *547*, 436.

(15) Roscoe, J. M.; Back, R. A. *J. Phys. Chem.* **1986**, *90*, 598.

(16) Khriachtchev, L. *J. Phys. Chem. A* **2015**, *119*, 2735.

(17) Sheridan, R. S. *J. Phys. Org. Chem.* **2010**, *23*, 326.

(18) Khriachtchev, L.; Domanskaya, A.; Marushkevich, K.; Räsänen, M.; Grigorenko, B.; Ermilov, A.; Andrijchenko, N.; Nemukhin, A. *J. Phys. Chem. A* **2009**, *113*, 8143.

(19) Zuev, P. S.; Sheridan, R. S.; Sauers, R. R.; Moss, R. A.; Chu, G. *Org. Lett.* **2006**, *8*, 4963.

(20) Han, S.; Yoo, H. S.; Kim, S. K. *J. Phys. Chem. A* **2010**, *114*, 10005.

(21) Choi, S.; Kang, T. Y.; Choi, K.-W.; Han, S.; Ahn, D.-S.; Baek, S. J.; Kim, S. K. *J. Phys. Chem. A* **2008**, *112*, 7191.

(22) Shivatare, V.; Tzeng, W. B. *Mol. Phys.* **2014**, *112*, 2397.

(23) Zhu, C.; Kais, S.; Zeng, X. C.; Francisco, J. S.; Gladich, I. *J. Am. Chem. Soc.* **2017**, *139*, 27.

(24) Zhang, J. L.; Zhong, J. Q.; Lin, J. D.; Hu, W. P.; Wu, K.; Xu, G. Q.; Wee, A. T. S.; Chen, W. *Chem. Soc. Rev.* **2015**, *44*, 2998.

(25) Tantirungrotechai, Y. *J. Mol. Struct.: THEOCHEM* **2003**, *624*, 279.

(26) Fahrenbach, A. C.; Bruns, C. J.; Cao, D.; Stoddart, J. F. *Acc. Chem. Res.* **2012**, *45*, 1581.

(27) Sauvage, J.-P.; Stoddart, J. F.; Feringa, B. L. *The Nobel Prize in Chemistry 2016*, http://www.nobelprize.org/nobel_prizes/chemistry/laureates/2016/press.html.

(28) Butz, K. W.; Krajnovich, D. J.; Parmenter, C. S. *J. Chem. Phys.* **1990**, *93*, 1557.

(29) Osamura, Y.; Schaefer, H. F. *J. Chem. Phys.* **1981**, *74*, 4576.

(30) Koch, D. M.; Khieu, N. H.; Peslherbe, G. H. *J. Phys. Chem. A* **2001**, *105*, 3598.

(31) Kuo, I. F. W.; Mundy, C. J. *Science* **2004**, *303*, 658.

(32) Jungwirth, P.; Tobias, D. J. *Chem. Rev.* **2006**, *106*, 1259.

(33) Gladich, I.; Shepson, P. B.; Carignano, M. A.; Szleifer, I. *J. Phys. Chem. A* **2011**, *115*, 5895.

(34) Gladich, I.; Habartova, A.; Roeselova, M. *J. Phys. Chem. A* **2014**, *118*, 1052.

(35) Vacha, R.; Jungwirth, P.; Chen, J.; Valsaraj, K. *Phys. Chem. Chem. Phys.* **2006**, *8*, 4461.

DOI: 10.1021/jacs.8b01503
J. Am. Chem. Soc. 2018, 140, 5535−5543

(36) Kania, R.; Malongwe, J. K.; Nachtigallova, D.; Krausko, J.; Gladich, I.; Roeselova, M.; Heger, D.; Klan, P. *J. Phys. Chem. A* **2014**, *118*, 7535.
(37) Olano, L. R.; Rick, S. W. *J. Comput. Chem.* **2005**, *26*, 699.
(38) van Maaren, P. J.; van der Spoel, D. *J. Phys. Chem. B* **2001**, *105*, 2618.
(39) Gladich, I.; Roeselova, M. *Phys. Chem. Chem. Phys.* **2012**, *14*, 11371.
(40) Dang, L. X. *J. Chem. Phys.* **1992**, *97*, 2659.
(41) Muchova, E.; Gladich, I.; Picaud, S.; Hoang, P. N. M.; Roeselova, M. *J. Phys. Chem. A* **2011**, *115*, 5973.
(42) Dorosh, O.; Kisiel, Z. *Acta Phys. Pol., A* **2007**, *112*, S-95.
(43) Hutter, J.; Iannuzzi, M.; Schiffmann, F.; VandeVondele, J. *Wiley Interdiscip. Rev. Comput. Mol. Sci.* **2014**, *4*, 15.
(44) Jämbeck, J. P. M.; Lyubartsev, A. P. *J. Phys. Chem. B* **2014**, *118*, 3793.
(45) Wang, J. M.; Wolf, R. M.; Caldwell, J. W.; Kollman, P. a.; Case, D. a. *J. Comput. Chem.* **2004**, *25*, 1157.
(46) Vácha, R.; Jungwirth, P.; Chen, J.; Valsaraj, K. *Phys. Chem. Chem. Phys.* **2006**, *8*, 4461.
(47) Hoehn, R. D.; Carignano, M. A.; Kais, S.; Zhu, C.; Zhong, J.; Zeng, X. C.; Francisco, J. S.; Gladich, I. *J. Chem. Phys.* **2016**, *144*, 214701.
(48) Jorgensen, W. L.; Chandrasekhar, J.; Madura, J. D.; Impey, R. W.; Klein, M. L. *J. Chem. Phys.* **1983**, *79*, 926.
(49) Bayly, C. I.; Cieplak, P.; Cornell, W. D.; Kollman, P. A. *J. Phys. Chem.* **1993**, *97*, 10269.
(50) Lamoureux, G.; Harder, E.; Vorobyov, I. V.; Roux, B.; MacKerell, A. D. *Chem. Phys. Lett.* **2006**, *418*, 245.
(51) Lemkul, J. A.; Roux, B.; van der Spoel, D.; MacKerell, A. D. *J. Comput. Chem.* **2015**, *36*, 1473.
(52) Abraham, M. J.; Murtola, T.; Schulz, R.; Páll, S.; Smith, J. C.; Hess, B.; Lindahl, E. *SoftwareX* **2015**, *1−2*, 19.
(53) Sprik, M.; Ciccotti, G. *J. Chem. Phys.* **1998**, *109*, 7737.
(54) Laio, A.; Gervasio, F. L. *Rep. Prog. Phys.* **2008**, *71*, 126601.
(55) Barducci, A.; Bussi, G.; Parrinello, M. *Phys. Rev. Lett.* **2008**, *100*, 020603.
(56) Iannuzzi, M.; Laio, A.; Parrinello, M. *Phys. Rev. Lett.* **2003**, *90*, 238302.
(57) Laio, A.; Parrinello, M. *Proc. Natl. Acad. Sci. U. S. A.* **2002**, *99*, 12562.
(58) Tribello, G. A.; Bonomi, M.; Branduardi, D.; Camilloni, C.; Bussi, G. *Comput. Phys. Commun.* **2014**, *185*, 604.
(59) Frisch, M. J.; Trucks, G. W.; Schlegel, H. B.; Scuseria, G. E.; Robb, M. A.; Cheeseman, J. R.; Scalmani, G.; Barone, V.; Mennucci, B.; Petersson, G. A.; Nakatsuji, H.; Caricato, M.; Li, X.; Hratchian, H. P.; Izmaylov, A. F.; Bloino, J.; Zheng, G.; Sonnenberg, J. L.; Hada, M.; Ehara, M.; Toyota, K.; Fukuda, R.; Hasegawa, J.; Ishida, M.; Nakajima, T.; Honda, Y.; Kitao, O.; Nakai, H.; Vreven, T.; Montgomery, J. A., Jr.; Peralta, J. E.; Ogliaro, F.; Bearpark, M. J.; Heyd, J.; Brothers, E. N.; Kudin, K. N.; Staroverov, V. N.; Kobayashi, R.; Normand, J.; Raghavachari, K.; Rendell, A. P.; Burant, J. C.; Iyengar, S. S.; Tomasi, J.; Cossi, M.; Rega, N.; Millam, N. J.; Klene, M.; Knox, J. E.; Cross, J. B.; Bakken, V.; Adamo, C.; Jaramillo, J.; Gomperts, R.; Stratmann, R. E.; Yazyev, O.; Austin, A. J.; Cammi, R.; Pomelli, C.; Ochterski, J. W.; Martin, R. L.; Morokuma, K.; Zakrzewski, V. G.; Voth, G. A.; Salvador, P.; Dannenberg, J. J.; Dapprich, S.; Daniels, A. D.; Farkas, Ö.; Foresman, J. B.; Ortiz, J. V.; Cioslowski, J.; Fox, D. J. *Gaussian09*; Gaussian, Inc.: Wallingford, CT, USA, 2009.
(60) Lee, C.; Yang, W.; Parr, R. G. *Phys. Rev. B: Condens. Matter Mater. Phys.* **1988**, *37*, 785.
(61) Becke, A. D. *J. Chem. Phys.* **1993**, *98*, 5648.
(62) Branduardi, D.; Bussi, G.; Parrinello, M. *J. Chem. Theory Comput.* **2012**, *8*, 2247.
(63) Gubskaya, A. V.; Kusalik, P. G. *J. Chem. Phys.* **2002**, *117*, 5290.
(64) Pekary, A. E. *J. Phys. Chem.* **1974**, *78*, 1744.

DOI: 10.1021/jacs.8b01503
J. Am. Chem. Soc. 2018, 140, 5535−5543